

TEMPERATURE DEVELOPMENT IN SCREW EXTRUDERS

By: Chris Rauwendaal and Giuseppe Ponzielli
REE, Inc. and RCT s.r.l.
Date: April 8, 2003

Introduction

Viscous dissipation and the resulting increase in melt temperature are important in most polymer extrusion operation. Existing theories do not allow a simple prediction of temperature development without resorting to numerical techniques. This paper describes the development of an analytical theoretical model that allows calculation of developing melt temperatures in a single screw extruder. The model based on simplified flow in screw extruders. Initially we consider only flow in the screw channel and assume the leakage flow through the flight clearance is negligible. The dissipation in the flight clearance is added later.

The polymer melt is considered as a power law fluid with a temperature dependent consistency index. We take into account viscous dissipation and heat transfer through the barrel; these are the main factors affecting the melt temperatures. As a result, the analytical results are useful in developing an understanding of the role of the different variables that affect the melt temperature development in the polymer extrusion process. The role of the power dissipated in the flight clearance is briefly discussed and a simple method to include this effect in the temperature calculations is presented. The effect of the flight clearance is significant for polymers that are not strongly shear thinning and for multi-flighted screws.

Power Consumption

The viscous dissipation of a power law fluid is determined from the consistency index (m), the shear rate ($\dot{\gamma}$), and the power law index (n). If we neglect the power consumed in the flight clearance the viscous dissipation can be written as:

$$q_s = m\dot{\gamma}^{n+1} = m\left(\frac{pDN}{H}\right)^{n+1} \quad (1)$$

We will take as an example an extruder screw with an outside diameter (D) of 60 mm, a channel depth (H) of 4 mm, a length (L) of $10D$, running at a rotational speed (N) of 100 rpm or 1.67 rev/sec. The polymer is a medium viscosity low density polyethylene with the following properties. The consistency index of the polymer is $m = 25120$ [Pa.sⁿ] and the power law index $n = 0.3$ [-]. With these data the power dissipation becomes $q_s = 7,324,273$ W/m³ (7,324.3 kW/m³). This is the specific power consumption per unit volume. The volume between the barrel and the screw can be approximated with:

$$V = pDHL \quad (2)$$

This means that the actual power consumption can be determined from:

$$Z = \frac{mL(pD)^{n+2} N^{n+1}}{H^n} \quad (3)$$

With a volume of $V = 0.0004524 \text{ m}^3$ the power consumption becomes $Z = 3,313.5 \text{ W} = 3.313 \text{ kW}$. This power consumption will result in an increase in melt temperature; this will be discussed next.

Temperature Increase

In order to determine the corresponding increase in melt temperature we need to know the specific heat and the melt density of the polymer. We will take the specific heat $C_p = 2,300 \text{ J/kg}^\circ\text{C}$ and the melt density $\rho = 750 \text{ kg/m}^3$. The adiabatic temperature rise (no heat transfer at the walls) can be determined as follows:

$$\Delta T_a = \frac{Z}{rC_p \dot{V}} = \frac{Z}{C_p \dot{M}} \quad (4)$$

where \dot{V} is the volumetric flow rate in axial direction and \dot{M} the mass flow rate. If we have a mass flow rate of 92.7 kg/hr (0.02574 kg/s) the adiabatic temperature rise is $\Delta T_a = 55.97^\circ\text{C}$. This mass flow rate is typical for a 60-mm extruder running at a screw speed of 100 rpm. As a result, we can expect a considerable increase in melt temperature by viscous dissipation over a length of $10D$. Equation 4 assumes that the shear rate is determined only by the tangential velocity differences in the extruder screw and that the axial velocity gradients are negligible for the determination of the melt temperature rise. These are generally reasonable assumptions for screw extruders.

The flow rate for screw extruders can be predicted from the following expression (1).

$$\dot{V} = 0.5(1 - r_t)WHv_{bz} = 0.5(1 - r_t)(pD)^2 HN \sin \mathbf{f} \cos \mathbf{f} \quad (5)$$

where r_t is the throttle ratio (pressure flow divided by drag flow), and ϕ is the flight helix angle.

With expression 5 we can express the adiabatic temperature rise as follows.

$$\Delta T_a = \frac{2mL}{rC_p H (1 - r_t) \sin \mathbf{f} \cos \mathbf{f}} \left(\frac{pDN}{H} \right)^n \quad (6)$$

From this expression the various parameters that influence the temperature rise by viscous dissipation can be clearly distinguished. The temperature rise increases with consistency index (m), the length (L), the screw diameter (D), the screw speed (N), and the power law index (n). The temperature rise reduces with melt density (ρ), the specific heat (C_p), the channel depth (H), the throttle ratio (r_t), the helix angle (ϕ).

Effect of Temperature Dependent Viscosity

The actual rise in melt temperature will generally be less than the values predicted by equations 4 and 6. One of the reasons for this is that the melt viscosity reduces with increasing temperature. The temperature dependence of the viscosity for a power law fluid can be written as follows.

$$h(T) = m_r \exp[a(T_r - T)] \dot{g}^{n-1} \quad (7)$$

This means that the consistency index is made temperature dependent using an exponential dependence of temperature with a temperature coefficient of a . The consistency index m_r is the value at reference temperature T_r .

Adiabatic Case (Dissipation without Conductive Heat Transfer)

We can determine the temperature rise over an infinitesimally small axial distance dx . This leads to the following differential equation.

$$\frac{dT}{dx} = B_1 m_r \exp[a(T_r - T)] \quad (8)$$

Constant B_1 can be written as:

$$B_1 = \frac{m_r (\rho D)^{n+2} N^{n+1}}{H^n C_p \dot{M}} \quad (9)$$

This differential equation can be solved with the boundary condition $T(x=0) = T_0$. The temperature as a function of axial distance x can now be written as:

$$T(x) = \frac{1}{a} \ln \left(e^{aT_0} + aB_1 x e^{aT_r} \right) \quad (10)$$

If we make the initial temperature $T_0 = 190^\circ\text{C}$ equal to the reference temperature and take the temperature coefficient to be $a = 0.02 \text{ }^\circ\text{C}^{-1}$ then the temperature after 10D becomes: $T(x=0.6) = 227.56^\circ\text{C}$. This means that the adiabatic temperature rise with a temperature dependent viscosity is 37.56°C compared to 55.97°C for a temperature independent viscosity. This indicates that temperature dependence of the viscosity results in a significantly lower temperature rise.

Figure 1 shows how the melt temperature changes over distance for several values of the temperature coefficient (a). For very low values of “ a ” the melt temperature increases linearly with distance. This corresponds to the temperature profile for a temperature independent fluid.

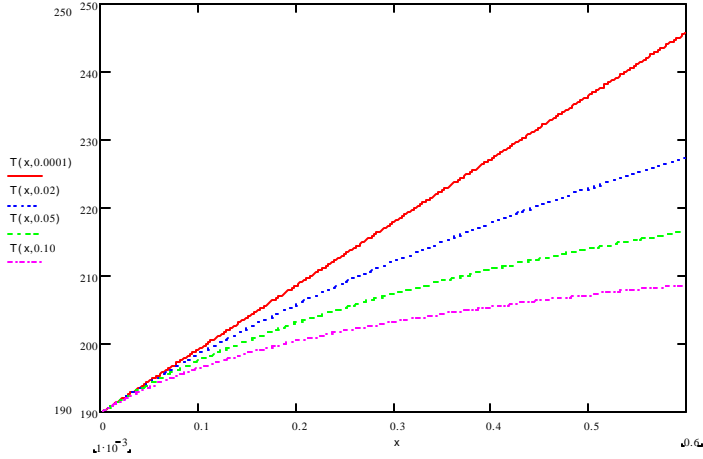


Figure 1, Melt temperature vs. distance for several values of temperature coefficient "a"

When the temperature coefficient increases the melt temperatures reduce. Most semi-crystalline polymers have a temperature coefficient of about 0.02; amorphous polymers generally have a temperature coefficient of about 0.05. Figure 1 shows that an increase in the temperature coefficient from 0.02 to 0.05 reduces the temperatures significantly, about 10°C after a length of 10D.

Effect of Screw Speed and Throttle Ratio

Figure 2 shows how the temperature development is affected by screw speed assuming adiabatic conditions.

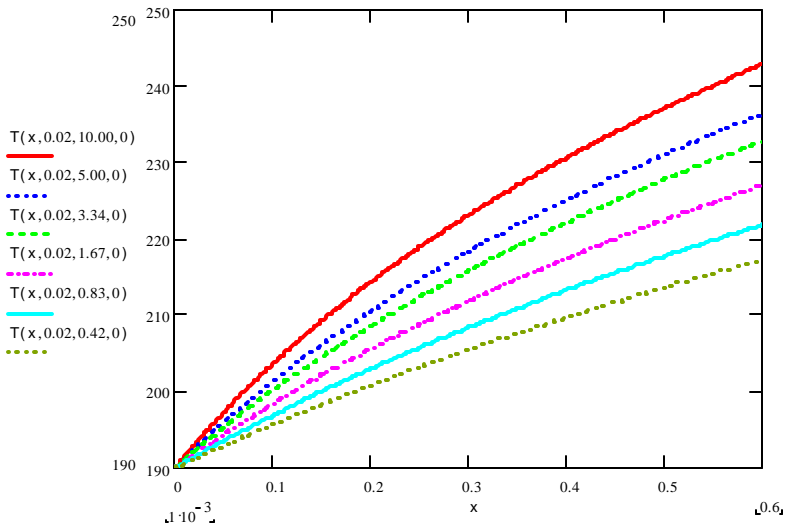


Figure 2, Temperature vs. distance for several values of the screw speed

The effect of increasing screw speed diminishes at higher screw speeds. Increasing the screw speed from 25 to 50 rpm increases the final temperature by about 5°C while an increase from 100 to 200 rpm increases the final temperature about 4°C.

Figure 3 shows how the temperature development is affected by the value of the throttle ratio again assuming adiabatic conditions. The values of the throttle ratio range from -0.5 to +0.5. The last number in the parentheses behind T represent the throttle ratio. For instance, $T(x, 0.02, 1.67, -0.5)$ means temperature (T) as a function of axial distance (x) at a temperature coefficient $a = 0.02$, a screw speed of $N = 1.67$ rev/sec, and a throttle ratio of $r_t = -0.5$. The lowest value of throttle ratio (-0.5) results in the lowest increase in melt temperature. Negative values of the throttle ratio correspond to a negative axial pressure gradient and a mass flow rate higher than the drag flow rate. Higher mass flow rates result in shorter residence times and, thus, in lower melt temperatures. When the polymer melt is exposed to a certain shear rate for a shorter time the resulting increase in melt temperature is reduced.

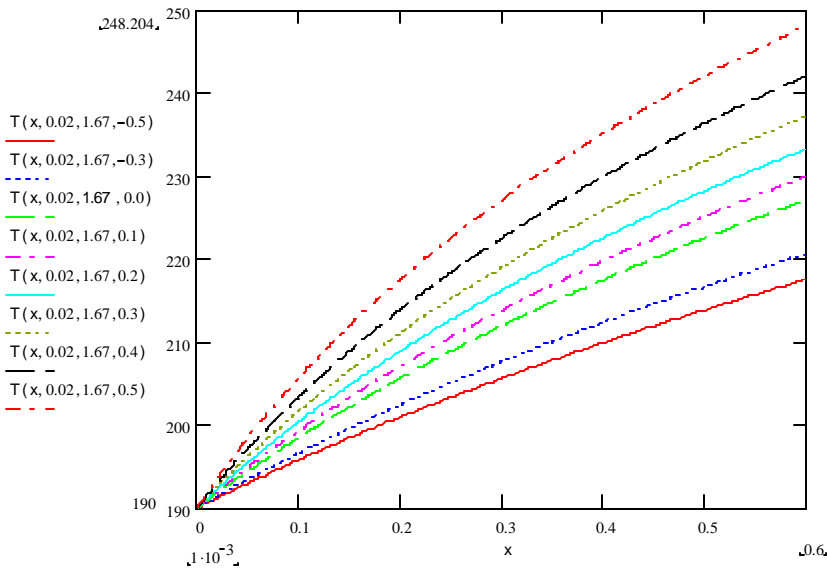


Figure 3, Temperature vs. distance for several values of the throttle ratio

When the throttle ratio is zero the mass flow rate equals the drag flow rate; in this case the axial pressure gradient is zero. When the throttle ratio is positive the axial pressure gradient is positive and the mass flow rate is less than the drag flow rate. This results in longer residence times and higher melt temperature.

Figure 4 shows how the adiabatic temperature development is affected by the value of the throttle ratio and the screw speed. The top curve is actually two curves almost completely overlapping. One curve corresponds to a screw speed of 1.67 rev/sec (100 rpm) and a throttle ratio of 0.4, the other curve corresponds to a screw speed of 9.3 rev/sec (558 rpm) and a throttle ratio of 0. The bottom curve is also two curves almost completely overlapping. One curve corresponds to a screw speed of 1.67 rev/sec (100

rpm) and a throttle ratio of -0.5, the other curve corresponds to a screw speed of 0.42 rev/sec (25 rpm) and a throttle ratio of 0.

These two sets of curves indicate that an increase in screw speed can be offset by a reduction in the throttle ratio. The throttle ratio is determined by the inlet and outlet pressure of the melt conveying zone. It is clear, therefore, that reducing barrel pressure will reduce polymer melt temperature. This can be achieved by using a less restrictive screen pack, a less restrictive extrusion die, higher die temperatures, or by using a melt pump to generate most of the diehead pressure.

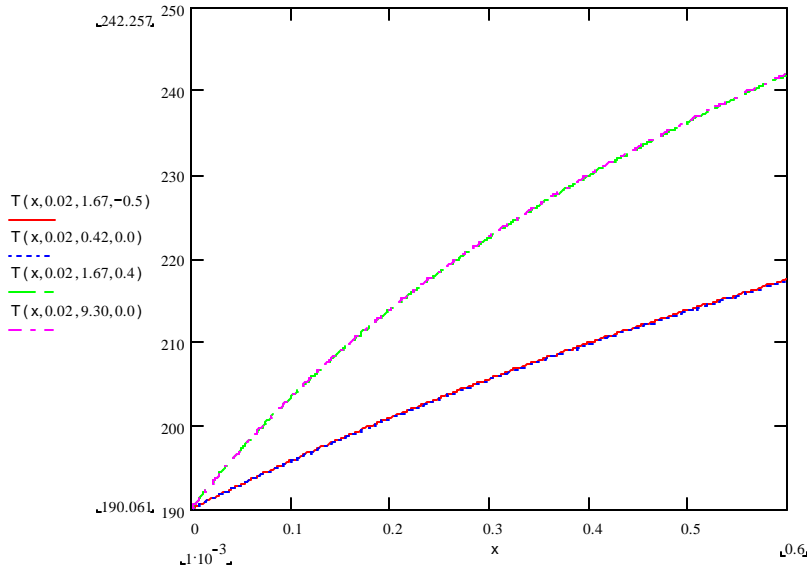


Figure 4, Temperature vs. distance for different values of screw speed and throttle ratio

Conductive Heat Transfer without Dissipation

We can also determine the temperature development for the case of zero viscous dissipation and non-zero conductive heat transfer. If the heat flux is determined by the temperature difference between the melt temperature T and the barrel coolant temperature T_c at distance h away from the barrel ID, the heat flux can be written as:

$$q_c = k_b \frac{T - T_c}{h} \quad (11)$$

where k_b is the thermal conductivity of the barrel.

The temperature gradient resulting from heat conduction can be expressed as:

$$\frac{dT}{dx} = -\frac{k(T - T_c) \rho D}{h C_p \dot{M}} = -A_2(T - T_c) \quad (12)$$

With boundary condition $T(x=0) = T_0$ the change in melt temperature resulting from conductive heat transfer can be written as:

$$\Delta T_c(x) = (T_0 - T_c)(e^{-A_2 x} - 1) \quad (13)$$

Expression 13 is useful for cases where the conductive heat transfer is important and the viscous heat generation negligible. In most realistic polymer extrusion operations both the viscous dissipation and the heat conduction are important. The combined effect of these factors will be discussed next.

Temperatures Development with Dissipation and Conduction

Expression 10 applies only to temperature development with viscous dissipation under adiabatic conditions, i.e. without heat transfer through the barrel or the screw. In reality, however, there will be conductive heat transfer through the barrel. If the heat transfer through the barrel is constant, the temperature gradient is determined by both viscous dissipation and conduction. In this case, the temperature gradient can be expressed as:

$$\frac{dT}{dx} = B_1 e^{a(T_r - T)} - B_2 \quad (14)$$

Constant B_1 is given by equation 9, constant B_2 is given by:

$$B_2 = \frac{q_c p D}{C_p M} \quad (15)$$

The units of B_1 and B_2 are [$^{\circ}\text{C}/\text{m}$]; these are units of temperature gradient. Constant B_1 represents the contribution of viscous heating and constant B_2 represents the contribution of conductive heat transfer. Variable q_c is the heat flux through the barrel wall. Subject to boundary condition $T(x=0) = T_0$ the differential equation can be solved. The solution can be written as:

$$T(x) = \frac{1}{a} \ln \left[\left(e^{aT_0} - \frac{B_1}{B_2} e^{aT_r} \right) e^{-aB_2 x} + \frac{B_1}{B_2} e^{aT_r} \right] \quad (16)$$

For very small values of B_2 the results of equation 16 become the same as the results of equation 10. As such equation 16 is a more general description of the developing temperature than equation 10.

Equation 16 allows determination of the thermal development length, x_{fd} . This is the axial distance necessary for the temperature to reach fully developed conditions, i.e. the temperature no longer changes with distance. Since the temperature gradient generally does not reach a zero value until x reaches infinity, it is more practical to define a thermal development length based on the distance at which the temperature gradient falls below a

certain value B_0 . We can set the value of this limiting temperature gradient at $B_0 = 10$ [$^{\circ}\text{C}/\text{m}$]. The fully developed temperature can be determined from equation 13:

$$B_0 = B_1 e^{a(T_r - T)} - B_2 \quad (17)$$

This leads to the following expression for the fully developed temperature:

$$T_{fd} = T_r - \frac{1}{a} \ln \frac{B_0 + B_2}{B_1} \quad (18)$$

When we insert this value of the temperature into equation 16 we can determine the thermal development length; this can be written as:

$$x_{fd} = -\frac{1}{aB_2} \ln \left[\left(\frac{B_0 B_1}{B_0 + B_2} \right) \left(\frac{e^{aT_r}}{B_1 e^{aT_r} - B_2 e^{aT_0}} \right) \right] \quad (19)$$

Expressions for the fully developed temperature were developed by Rauwendaal (3). However, the equation 18 yields more accurate results because it takes into account the temperature dependence of the viscosity as well as the shear thinning behavior of the polymer melt.

Temperature Profiles with Dissipation and Conduction

With expressions 14-19 we can evaluate the combined effect of conduction and viscous dissipation on the temperature development. Figure 5 shows the temperature profiles for different screw speeds (0.42, 0.83, 1.67, 3.34, 5.00, and 10.00 rev/sec) with a heat flux of $-10,000 \text{ W}/\text{m}^2$. The results of figure 5 can be compared to those of figure 3 that do not include the effect of conduction.

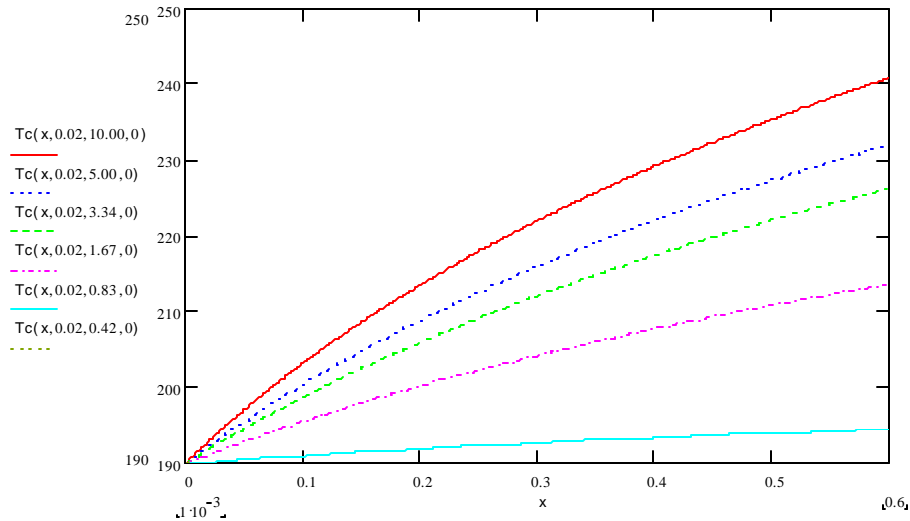


Figure 5, Temperature profiles at different screw speeds with heat flux of $-10,000 \text{ W/m}^2$

Comparison of figure 5 to figure 3 shows that the melt temperatures reduce when conduction is taken into account and the heat flux is negative (i.e. the melt is cooled). The reduction in melt temperature is small for high screw speed. However, the reduction in temperature becomes significant at lower screw speed. At 100 rpm with a heat flux of $-10,000 \text{ W/m}^2$ the melt temperature drops about $14 \text{ }^\circ\text{C}$ to about $214 \text{ }^\circ\text{C}$.

Figure 6 shows the temperature profiles at three different screw speeds with and without conduction; the heat flux is $-10,000 \text{ W/m}^2$. At a screw speed of 10 rev/sec (600 rpm) the temperature drops about $2 \text{ }^\circ\text{C}$ after a distance of 10D. At a screw speed of 3.34 rev/sec (200 rpm) the melt temperature drops about $6.5 \text{ }^\circ\text{C}$ and at 0.83 rev/sec (50 rpm) the melt temperature drops about $27 \text{ }^\circ\text{C}$. Clearly, at low screw speed the melt temperature can be affected significantly by conduction through the barrel. The reason for the large effect of barrel cooling at low screw speed is that the residence time of the polymer increases with reducing screw speed. As a result, more time is available to remove heat from the polymer melt at low screw speed.

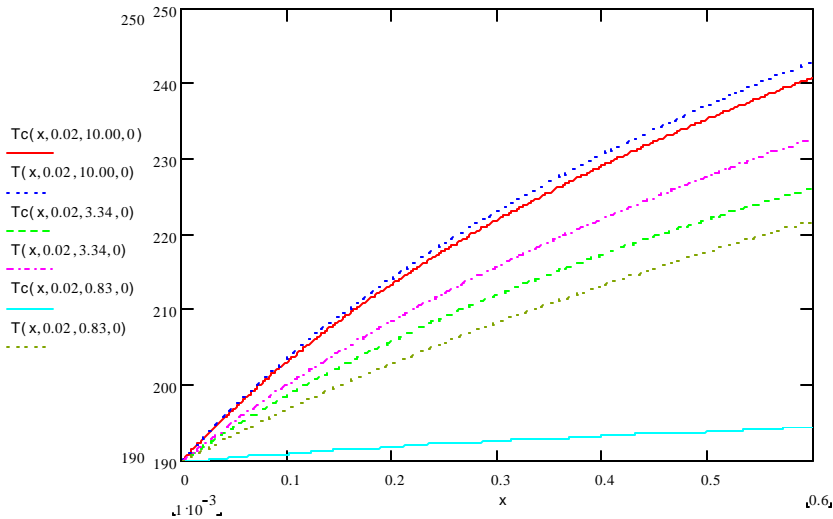


Figure 6, Temperature profiles at different screw speed with and without heat transfer (T is the temperature without heat transfer and T_c is the temperature with heat transfer)

The thermal development length is plotted against screw speed in figure 7 at several values of the temperature coefficient. The heat flux at the barrel is set at $-10,000 \text{ W/m}^2$ and the value of B_0 is set at $10 \text{ }^\circ\text{C/m}$. This figure clearly shows that the thermal development length reduces with increasing values of the temperature coefficient. This is to be expected because increasing values of the temperature coefficient reduce the amount of viscous dissipation when the temperature goes up.

For the case shown in figure 7 the thermal development length becomes longer than the typical metering section of an extruder when the screw speed is greater than about 1 rev/sec (60 rpm). This means that at high screw speeds it cannot be expected that the melt temperatures become fully developed within the length of the extruder.

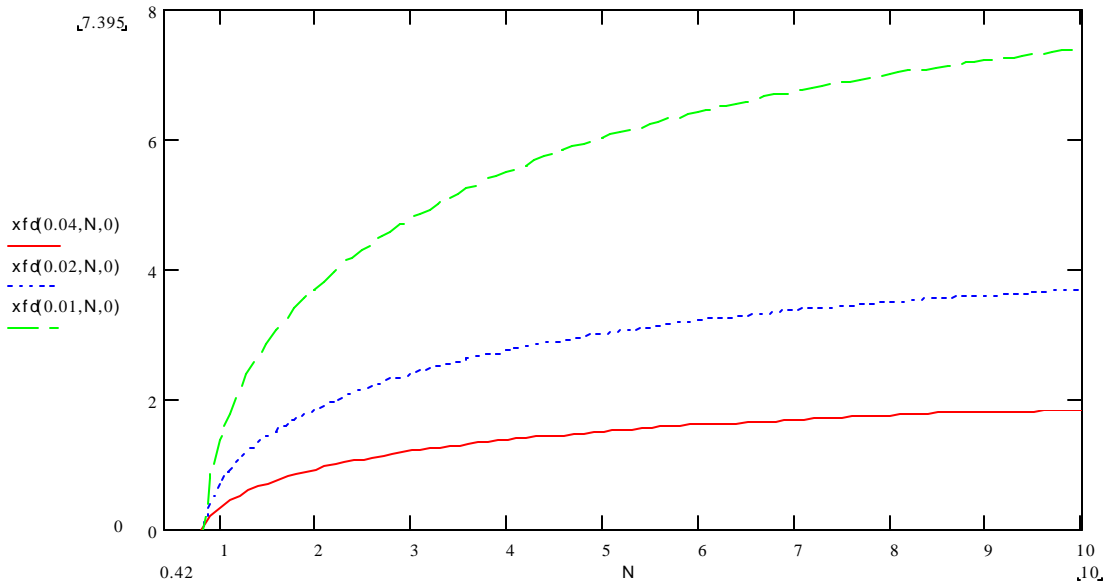


Figure 7, Thermal development length versus screw speed

Figure 7 shows that the thermal development length becomes zero at a screw speed of about 0.7 rev/sec. It is evident from equation 19 that the thermal development length is zero when $B_1 = (B_2 + B_0)\exp[a(T_0 - T_r)]$. From this relationship we can determine the screw speed at which the thermal development length becomes zero.

$$N_0 = \left[\frac{\dot{M} C_p H^n}{m_r (\rho D)^{n+2}} \left(B_0 + \frac{q_c \rho D}{C_p \dot{M}} \right) e^{a(T_0 - T_r)} \right]^{\frac{1}{n+1}} \quad (20)$$

When B_0 is taken as zero equation 20 represents the screw speed at which the viscous dissipation equals the heat transfer. At this critical screw speed the melt temperature does not change at all along the length of the extruder screw. This critical value of the screw speed is not dependent on the mass flow rate and specific heat; it can be written as:

$$N_{crit} = \left[\frac{q_c H^n e^{a(T_0 - T_r)}}{m_r (\rho D)^{n+1}} \right]^{\frac{1}{n+1}} \quad (21)$$

Thus, the critical screw speed depends on the heat flux, channel depth, temperature coefficient, initial melt temperature, reference temperature, consistency index, screw diameter, and power law index. The critical screw speed increases with the heat flux and channel depth and reduces with the power law index, consistency index, and screw diameter. The effect of the power law index is shown in figure 8.

Even relatively small increases in the power law index, e.g. from 0.3 to 0.5, can reduce the critical screw speed significantly. This indicates that small increases in power law index can cause significant increases in viscous heating and melt temperature. This is known in practice when we consider the extrusion characteristics of LLDPE relative to LDPE (2). The power law index of LLDPE is considerably higher than that of LDPE. As a result, LLDPE tends to have more power consumption, higher melt temperatures, higher diehead pressures, and is more susceptible to melt fracture.

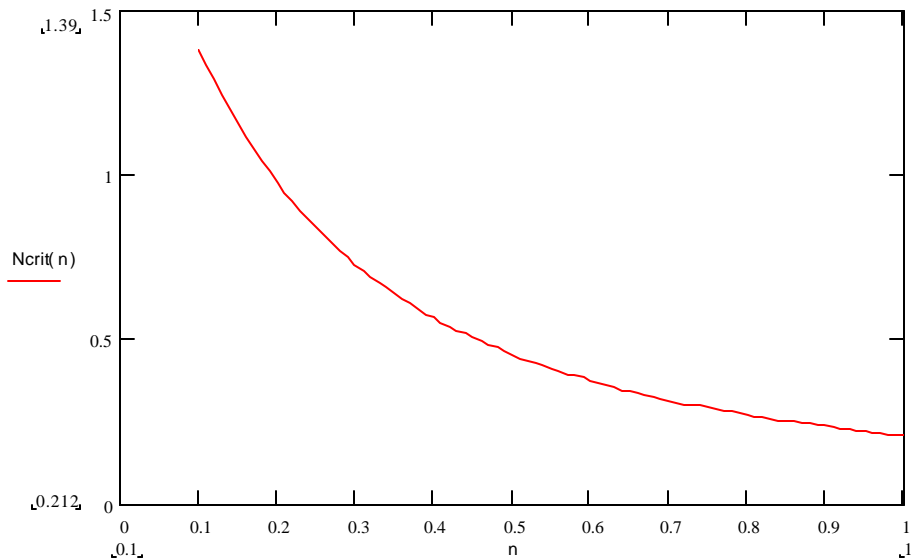


Figure 8, Critical screw speed versus power law index for heat flux of 10,000 W/m²

Equation 21 can be rewritten to determine the critical heat flux that is necessary to carry away the heat generated by viscous dissipation. This critical heat flux can be written as:

$$q_{c-crit} = \frac{m_r (pDN)^{n+1}}{H^n e^{a(T_0 - T_r)}} \quad (22)$$

This equation indicates that the amount of cooling necessary to maintain constant melt temperature increases with the consistency index, screw diameter, screw speed, and power law index. The critical heat flux reduces with increasing channel depth and temperature coefficient. Equation 22 provides a practical tool to determine the cooling capacity required to remove the amount of heat generated by viscous dissipation.

Comparison to Numerical Calculations

To compare the results of the analytical solutions to numerical calculations several simulations were performed with a 60-mm square pitch extruder screw using the Compuplast Flow 2000 simulation software. Figure 9 shows the increase in melt temperature over the length of a 10D long screw with an OD of 60-mm and a channel depth of 4 mm. The polymer melt flow properties are the same as used in the earlier example. The temperature field is shown as a color contour plot.

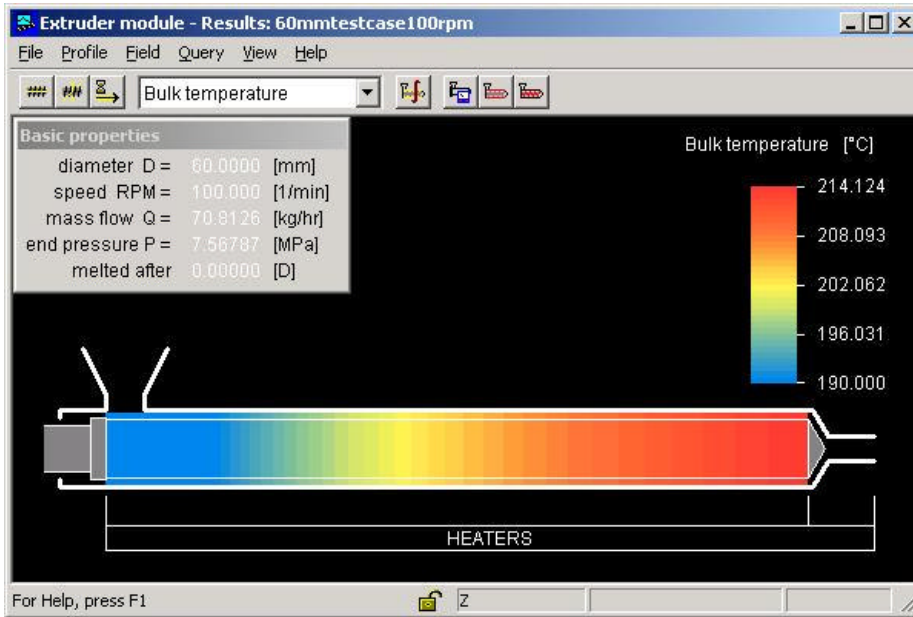


Figure 9, Melt temperature field for 60-mm extruder at 100 rpm

Figure 9 shows that the increase in melt temperature is about 24°C. The adiabatic temperature rise (equation 10) is about 37°C. The difference between these two values is largely due to the fact that the numerical predictions include heat transfer to the barrel. The heat flux (q_c) calculated in the numerical simulation is about $q_c = -10,000 \text{ W/m}^2$. Considering that the total heat transfer area (πDL) is 0.113 m^2 the total heat loss is about 1,130 W. We can relate this heat loss with a reduction in melt temperature by conductive heat transfer.

$$\Delta T_c = \frac{q_c pDL}{C_p \dot{M}} \quad (23)$$

The reduction in melt temperature from this heat loss is about 19°C. This explains to a large extent the difference in predicted melt temperatures comparing the analytical solution to the numerical solution.

The temperature rise with dissipation and heat conduction (equation 16) is about 23°C with a heat flux of $-10,000 \text{ W/m}^2$, see figure 5 with screw speed of 1.67 rev/sec (100 rpm). These results compare favorably to the numerical results; thus, the analytical solutions correspond closely to the numerical calculations.

Figure 10 shows the numerical predictions of melt temperature and pressure along the length of the extruder as a simple line graph. This graph can be compared to figure 5; it shows that the predicted temperature profiles show a pattern similar to that shown in figure 10. This indicates that the analytical expressions appear to yield reasonable results.

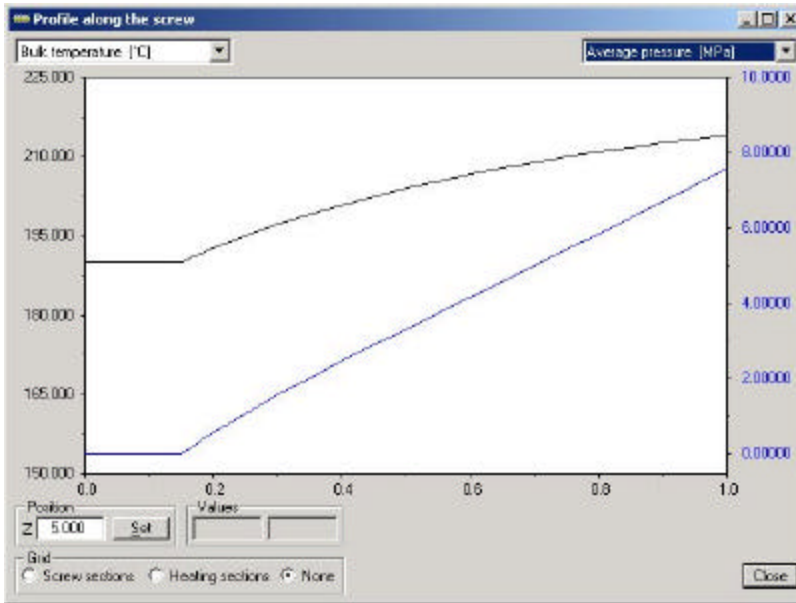


Figure 10, Melt temperature and pressure profiles along the length of the extruder

The heat flux may not be constant along the length of the extruder. In this case, the temperature profiles in different sections of the extruder may have to be determined separately to take into account different heat fluxes in different parts of the extruder. The same is true if the screw geometry changes along the length of the melt conveying part of the screw.

Discussion

The expressions derived in this paper allow a realistic calculation of developing melt temperatures along an extruder screw. Many authors have studied developing melt temperatures, e.g. (4-6); however, closed-form analytical solutions as presented in this paper have not been published before. Most realistic calculations of developing melt temperatures in screw extruders require numerical analysis. For instance, Derezinski solved the problem numerically with the barrel temperature as the boundary condition and a power-law viscosity (14). Later the analysis was extended to include a Carreau-Yasuda viscosity model(15).

Heat transfer through extruder barrels has been discussed by a number of authors as well, e.g. (7-11). The expressions developed in this paper allow determination of axial temperature profiles if the heat transfer rate through the barrel is known. With good instrumentation on an extruder it is possible to determine the amount of heat removed through the barrel.

It should be noted that the melt temperatures calculated in this paper represent the bulk average temperature at a certain axial location along the extruder screw. At a certain cross section the melt temperatures will vary in both radial and circumferential direction.

In order to predict both the axial and the cross sectional temperature profiles a 3D analysis has to be performed (e.g. 12). Such analyses invariably requires numerical techniques to solve the pertinent equations.

The analysis as developed to this point assumes that the effect of flight clearance is negligible. This assumption is not unreasonable for the prediction of melt temperature as long as the flight clearance is small so that the flight provides an efficient wiping action (13). However, this assumption is less reasonable for the prediction of power consumption (equation 3) because a significant amount of power can be dissipated in the flight clearance. This is particularly true for polymers with relatively high values of the power law index, i.e. weakly shear thinning materials.

Equation 3 can be expanded to take into account the power dissipated in the flight clearance. This leads to the following expression:

$$Z = Z_c + Z_f \quad (24)$$

where the power consumed in the channel is given by:

$$Z_c = \frac{mL_c (\mathbf{p}D)^{n+2} N^{n+1}}{H^n} \quad (25)$$

and the power consumed in the flight clearance is given by:

$$Z_f = \frac{mL_f (\mathbf{p}D)^{n+2} N^{n+1}}{\mathbf{d}^n} \quad (26)$$

where \mathbf{d} is the radial flight clearance, L_c the axial channel length, and L_f the axial flight length.

Equations 24-26 allow a more realistic calculation of the power consumption. The melt temperature rise in the flight clearance is generally small because the heat is effectively conducted away due to the fact that the clearance melt film thickness is very small compared to the channel depth (13). With equations 24-26 the total power consumption can be written as:

$$Z = m(\mathbf{p}D)^{n+2} N^{n+1} \frac{L_c}{H^n} \left(1 + \frac{L_f}{L_c} \frac{H^n}{\mathbf{d}^n} \right) \quad (27)$$

Usually the axial flight length is about one-tenth of the channel length ($L_f = 0.1 L_c$) and the flight clearance is about 2% of the channel depth ($\mathbf{d} = 0.02H$). With these numbers the power consumed in the flight clearance is about 30% of the power consumed in the channel when $n = 0.3$, about 70% when $n = 0.5$, and about 150% when $n = 0.7$. Clearly, for values of the power law index over 0.3 the power consumption in the clearance

cannot be neglected in most cases. For multi-flighted screws the power consumed in the flight clearance is even more significant and certainly not negligible.

The bracketed term on the right hand side of equation 27 can be used to as a correction term in equations 4-23 to incorporate the effect of the power dissipated in the flight clearance. Obviously, for polymers with a relatively large value of the power law index the correction can be significant.

Conclusions

This paper describes the derivation of analytical expressions of developing melt temperatures in screw extruders. The analytical expressions for temperature as a function of axial distance are useful in predicting axial melt temperature profiles. The advantage of analytical expressions is that the factors influencing temperature development can be easily identified and their effect determined in a quantitative fashion. Both the temperature and shear rate dependence of the viscosity strongly effect the developing temperatures in the extruder.

The analytical predictions compare well to numerical predictions. This indicates that the analytical expressions can be useful in the analysis of melt temperature development in single screw extruders. The results indicate that the melt temperatures can become fully developed if the heat flux through the barrel is substantial and if the screw speed is not too high. When the screw speed is high and the consistency index large it is not likely that the melt temperatures will be fully developed at the discharge end; this is particularly true for large diameter extruders.

References

1. C. Rauwendaal, "Polymer Extrusion," 4th edition, *Carl Hanser Verlag*, München (2001)
2. C. Rauwendaal, "Analysis of Extrusion Characteristics of LLPDE," *Conference Proceedings, 41st SPE ANTEC*, Chicago, IL, 151-154 (1983)
3. C. Rauwendaal, "Estimating Fully Developed Melt Temperature in Extrusion," *Conference Proceedings, 58th SPE ANTEC*, Orlando, FL, 307-311, (2000)
4. I. Sbarski, E. Kosior, and S. Bhattacharya, "Temperature Rise in the Extrusion of Highly Viscous Composite Materials," *International Polymer Processing*, XII, 4, p. 341 (1997)
5. H. Ockendon and J.R. Ockendon, "Variable Viscosity Flows in Heated and Cooled Channels," *J. Fluid Mech.*, Vol. 83, p. 177-190 (1977)
6. T.H. Sun, "Variable Viscosity Flow in Heated and Cooled Channel with Internal Viscous Dissipation," *Advances in Polymer Technology*, Vol. 8, No. 1, p. 1-4 (1988)
7. W.M. Davis, "Heat Transfer in Extruder Reactors," *Chemical Engineering Progress*, November, p. 35-42 (1988), also Chapter 7 in "Reactive Extrusion, Principles and Practice, M. Xanthos, Editor, *Carl Hanser Verlag*, München (1992)
8. W.A. Kramer, "Extruder Barrel Cooling," *Conference Papers, 45th SPE ANTEC* (1987)

9. C.D Han, "Analysis of the Performance of a Cooling Extruder in Thermoplastic Foam Extrusion, *Conference Proceedings, 45th SPE ANTEC* (1987)
10. J.L. Radovich, "An Experimental Comparison of Heat Removal in Water or Air Cooled Aluminum Barrel Coolers," *TAPPI Polymers, Laminations &Coatings Conference*, 103-107 (1995)
11. E. Steward and B. Kramer, "Air versus Water Cooled Single Screw Extruders, Technical Papers, *Conference Proceedings, 61st SPE ANTEC* (2003)
12. J. Anderson and C. Rauwendaal, "Finite Element Analysis of Flow in Extruders," *Conference Proceedings, 52nd SPE ANTEC*, 298-305 (1994)
13. C. Rauwendaal, "Leakage Flow in Screw Extruders," *Doctoral Thesis, Twente University of Technology*, Department of Mechanical Engineering-Polymer Processing, the Netherlands (1988)
14. S. Derezinski, "Dimensionless Curves for Extruder Melt Temperature and Flow," *Conference Proceedings, 45th ANTEC*, Society of Plastic Engineers, May 1987, pp. 98-102 (1987)
15. S. Derezinski, "Heat Transfer Coefficients in Extruder Melt Sections," *Conference Proceedings, 54th ANTEC*, Society of Plastic Engineers, May 1996, pp. 417-421 (1996)